

CCD *UBV* photometric study of five open clusters - Dolidze 36, NGC 6728, NGC 6800, NGC 7209, and Platais 1

Z. F. Bostancı¹ • T. Yontan² • S. Bilir¹ • T. Ak¹
 • T. Güver^{1,3} • S. Ak¹ • E. Paunzen⁴ •
 Ç. S. Başaran² • E. Vurgun² • B. A. Akti² •
 M. Çelebi² • H. Ürgüp²

Z. F. Bostancı

¹Istanbul University, Faculty of Science, Department of Astronomy and Space Sciences, 34119, University, Istanbul, Turkey

T. Yontan

²Istanbul University, Institute of Graduate Studies in Science and Engineering, Programme of Astronomy and Space Sciences, 34116, Beyazıt, Istanbul, Turkey

S. Bilir

¹Istanbul University, Faculty of Science, Department of Astronomy and Space Sciences, 34119, University, Istanbul, Turkey

T. Ak

¹Istanbul University, Faculty of Science, Department of Astronomy and Space Sciences, 34119, University, Istanbul, Turkey

T. Güver

¹Istanbul University, Faculty of Science, Department of Astronomy and Space Sciences, 34119 University, Istanbul, Turkey

³Istanbul University Observatory Research and Application Center, Beyazıt, 34119, Istanbul, Turkey

S. Ak

¹Istanbul University, Faculty of Science, Department of Astronomy and Space Sciences, 34119, University, Istanbul, Turkey

E. Paunzen

⁴Department of Theoretical Physics and Astrophysics, Masaryk University, Kotlářská 2, 611 37 Brno, Czech Republic

Ç. S. Başaran

²Istanbul University, Institute of Graduate Studies in Science and Engineering, Programme of Astronomy and Space Sciences, 34116, Beyazıt, Istanbul, Turkey

E. Vurgun

²Istanbul University, Institute of Graduate Studies in Science and Engineering, Programme of Astronomy and Space Sciences,

Abstract In this study, we present CCD *UBV* photometry of poorly studied open star clusters, Dolidze 36, NGC 6728, NGC 6800, NGC 7209, and Platais 1, located in the first and second Galactic quadrants. Observations were obtained with T100, the 1-m telescope of the TÜBİTAK National Observatory. Using photometric data, we determined several astrophysical parameters such as reddening, distance, metallicity and ages and from them, initial mass functions, integrated magnitudes and colours. We took into account the proper motions of the observed stars to calculate the membership probabilities. The colour excesses and metallicities were determined independently using two-colour diagrams. After obtaining the colour excesses of the clusters Dolidze 36, NGC 6728, NGC 6800, NGC 7209, and Platais 1 as 0.19 ± 0.06 , 0.15 ± 0.05 , 0.32 ± 0.05 , 0.12 ± 0.04 , and 0.43 ± 0.06 mag, respectively, the metallicities are found to be 0.00 ± 0.09 , 0.02 ± 0.11 , 0.03 ± 0.07 , 0.01 ± 0.08 , and 0.01 ± 0.08 dex, respectively. Furthermore, using these parameters, distance moduli and age of the clusters were also calculated from

34116, Beyazıt, Istanbul, Turkey

B. A. Akti

²Istanbul University, Institute of Graduate Studies in Science and Engineering, Programme of Astronomy and Space Sciences, 34116, Beyazıt, Istanbul, Turkey

M. Çelebi

²Istanbul University, Institute of Graduate Studies in Science and Engineering, Programme of Astronomy and Space Sciences, 34116, Beyazıt, Istanbul, Turkey

H. Ürgüp

²Istanbul University, Institute of Graduate Studies in Science and Engineering, Programme of Astronomy and Space Sciences, 34116, Beyazıt, Istanbul, Turkey

colour-magnitude diagrams simultaneously using PARSEC theoretical models. The distances to the clusters Dolidze 36, NGC 6728, NGC 6800, NGC 7209, and Platais 1 are 1050 ± 90 , 1610 ± 190 , 1210 ± 150 , 1060 ± 90 , and 1710 ± 250 pc, respectively, while corresponding ages are 400 ± 100 , 750 ± 150 , 400 ± 100 , 600 ± 100 , and 175 ± 50 Myr, respectively. Our results are compatible with those found in previous studies. The mass function of each cluster is derived. The slopes of the mass functions of the open clusters range from 1.31 to 1.58, which are in agreement with Salpeter’s initial mass function. We also found integrated absolute magnitudes varying from -4.08 to -3.40 for the clusters.

Keywords Galaxy: open cluster and associations: individual: Dolidze 36, NGC 6728, NGC 6800, NGC 7209, Platais 1 – stars: Hertzsprung Russell (HR) diagram

1 Introduction

Open star clusters are important tools to study Galactic chemical composition and structure, dynamical evolution and star formation processes in the Galaxy. Since their members are formed within a few millions years simultaneously from the same molecular cloud, they are almost at the same age and distance with comparable chemical composition, but different stellar masses. Hence, open clusters give us great opportunity to determine structural and astrophysical parameters of a group of stars such as reddening, distance, metallicity, age, and then mass function, integrated magnitudes and colours.

In this context, we studied CCD *UBV* stellar photometry of five open clusters (Dolidze 36, NGC 6728, NGC 6800, NGC 7209, and Platais 1, see Table 1) located in the first and second Galactic quadrants and investigated their basic astrophysical parameters (reddening, distance, metallicity and age) as well as initial mass functions, integrated magnitudes and colours in detail. We used the technique that is based on the analysis of the two-colour diagrams (TCDs) and colour-magnitude diagrams (CMDs) of member stars of the clusters (cf. Bica et al. 2006; Yontan et al. 2015)

CCD *UBV* photometry of most of the clusters in our sample have not been examined closely in previous studies. We present physical parameters of the five open clusters inferred in previous studies from the literature to date in Table 1. Our paper is organized as follows. We briefly define the observations and reductions in Section 2. We then give the CMDs of the five open clusters and the membership probabilities of the stars in the respective fields in Section 3. We obtain the astrophysical parameters of each cluster in Section 4 and summarize our conclusions in Section 5.

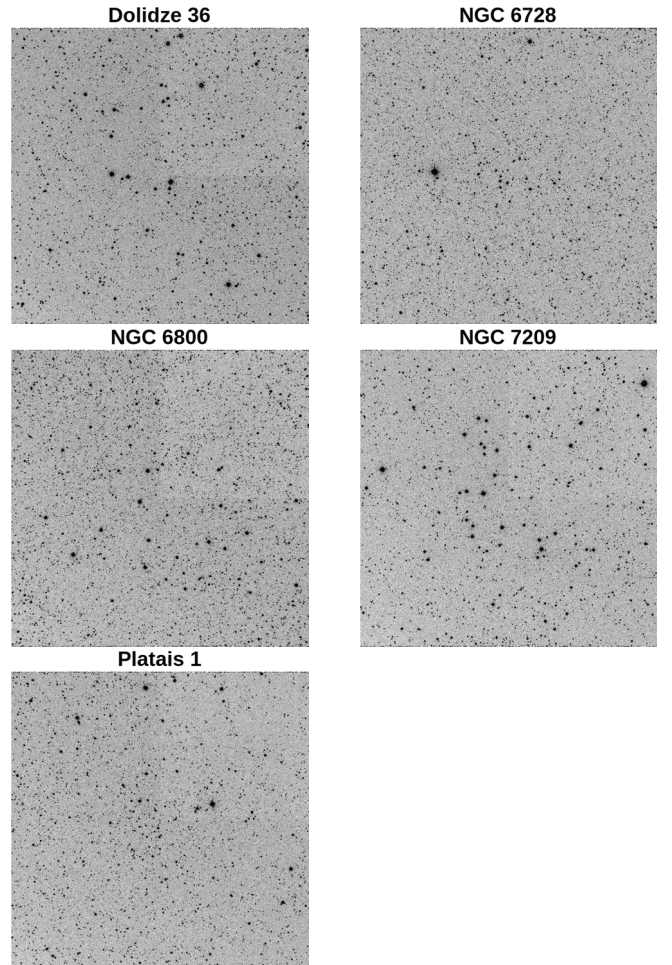


Fig. 1 Inverse coloured *V*-band images of five open clusters taken with T100 telescope. The field of view is about 21×21 arcmin (North top and East left).

Table 1 Galactic coordinates (l , b), colour excesses ($E(B - V)$), distance moduli (μ_V), distances (d), iron abundance ($[\text{Fe}/\text{H}]$), and age (t) collected from the literature for five open clusters under investigation. The references are given in the last column.

Cluster	l ($^\circ$)	b ($^\circ$)	$E(B - V)$ (mag)	μ_V (mag)	d (pc)	$[\text{Fe}/\text{H}]$ (dex)	$\log t$	References
Dolidze 36	77.66	+5.98	0.22	10.45	900	—	8.83	Kharchenko et al. (2005)
NGC 6728	25.76	-5.70	0.19±0.06	10.70±0.19	1050±90	0.00±0.09	8.60±0.10	This study
			0.15	10.47	1000	—	8.93	Kharchenko et al. (2005)
NGC 6800	59.23	+3.95	0.15±0.05	11.50±0.25	1610±190	0.02±0.11	8.88±0.08	This study
			0.40	11.29	1025	—	8.40	Ananjevskaia et al. (2015)
NGC 7209	95.50	-7.34	0.40	11.24	1000	—	8.59	Kharchenko et al. (2005)
			0.32±0.05	11.40±0.26	1210±150	0.03±0.07	8.60±0.10	This study
			0.16	10.83	1167	—	8.65	Kharchenko et al. (2005)
			0.171	10.60±0.06	1026±30	-0.07±0.03	8.65	Vansevicus et al. (1997)
			0.173	—	1095	—	8.48	Malysheva (1997)
			0.17	10.75	1140	0.07±0.05	—	Twarog et al. (1997)
			0.15±0.04	10.25	900	-0.01±0.11	8.48	Claria et al. (1996); Lynga (1987)
Platais 1	92.56	-1.65	0.15	—	900	-0.12	8.48	Piatti et al. (1995); Lynga (1987)
			0.12±0.04	10.50±0.18	1060±90	0.01±0.08	8.78±0.07	This study
			0.43±0.02	12.30±0.02	1568±13	—	8.04-8.28	Turner et al. (1994)
			0.43±0.06	12.50±0.29	1710±250	0.01±0.08	8.24±0.11	This study

Table 2 Log of observations with dates and exposure times for each passband. N refers to the number of exposure.

Cluster	Observation Date	Filter / (Exposure Time (s) \times N)		
		U	B	V
Dolidze 36	17.08.2012	90 \times 3, 360 \times 3	5 \times 3, 60 \times 3	3 \times 3, 30 \times 4
NGC 6728	19.07.2012	3 \times 3, 60 \times 1, 120 \times 2	0.6 \times 3, 1 \times 1, 25 \times 4	0.25 \times 3, 7 \times 3
NGC 6800	20.07.2012	90 \times 3, 360 \times 3	5 \times 3, 60 \times 3	3 \times 3, 30 \times 2
NGC 7209	16.08.2012	60 \times 3, 360 \times 3	5 \times 3, 60 \times 3	2 \times 3, 20 \times 3
Platais 1	08.08.2013	60 \times 3	4 \times 3	2 \times 4

2 Observations

CCD UBV observations of the five open clusters were performed with the 1-m Ritchey-Chrétien telescope (T100) of the TÜBİTAK National Observatory (TUG)¹ located in Turkey. Inverse coloured V -band images of the clusters are given in Fig. 1. Each frame contains an integrated image of the largest exposure obtained.

Cluster images were taken using a Spectral Instruments (SI 1100) CCD camera operating at -90°C . The camera is equipped with a back illuminated 4k \times 4k pixels CCD, with a pixel scale of 0.''31 pixel⁻¹, resulting in an unvignetted field of view of about 21' \times 21'. The readout noise and the gain of the CCD camera is 4.19 e⁻ and 0.55 e⁻/ADU, respectively. In order to be sensitive to the widest possible flux range, different exposure times were used during the observations. A log of observations is given in Table 2. Due to poor seeing it was not possible to use long exposure data of Platais 1. IRAF², PyRAF³ and astrometry.net⁴

(Lang et al. 2010) routines were used together with our own scripts for CCD calibrations as well as the astrometric corrections of the images. In order to determine atmospheric extinction and transformation coefficients for each night, we observed several star fields containing more than one Landolt (2009)'s standard stars. We took three images per band for each field and some fields could be observed several times. Details of the observations are given in Table 3. Instrumental magnitudes of the standard stars were measured with the aperture photometry packages of IRAF while brightness of the objects in cluster fields were obtained with Source Extractor and PSF Extractor routines (Bertin & Arnouts 1996). Applying multiple linear fits to the instrumental magnitudes of the standard stars, we obtained the photometric extinction and transformation coefficients for each night. We list the extinction coefficients and transformation coefficients for the individual nights in Table 4. After the application of aperture correction to instrumental magnitudes, stellar magnitudes were obtained with transformation equations given in previous studies (Janes & Hoq 2013; Yontan et al. 2015).

¹www.tug.tubitak.gov.tr

²IRAF is distributed by the National Optical Astronomy Observatories

³PyRAF is a product of the Space Telescope Science Institute, which is operated by AURA for NASA

⁴http://astrometry.net

Table 3 Observations of Landolt (2009)'s standard star fields, Field name (Field), number of stars (N_{st}), number of pointings to the fields (N_{obs}), airmass range for all fields (X_{range}) are given.

Date	Field	N_{st}	N_{obs}	X_{range}
19.07.2012	PG1530+057	3	1	1.184 - 2.571
	PG2213-006	7	1	
	SA110	10	1	
	SA111	5	1	
	SA112	6	10	
	SA113	15	1	
20.07.2012	SA114	5	1	1.183 - 2.612
	PG1530+057	3	1	
	SA110	10	1	
	SA111	5	1	
16.08.2012	SA112	6	5	1.164 - 3.196
	F24	4	1	
	G93	5	11	
	PG1633+099	8	1	
	PG2213-006	7	1	
	SA108	2	1	
	SA110	10	1	
	SA112	6	1	
	SA92	6	1	
SA93	4	1		
17.08.2012	F24	4	1	1.182 - 2.889
	G93	5	15	
	PG1633+099	8	1	
	PG2213-006	7	1	
	SA108	2	1	
	SA110	10	1	
	SA112	6	1	
	SA92	6	1	
	SA93	4	1	
08.08.2013	F11	3	1	1.153 - 2.466
	G93	5	2	
	GD246	4	1	
	PG2213-006	7	1	
	SA107	7	1	
	SA111	5	1	
	SA112	6	6	
	SA113	15	1	
	SA114	5	1	
SA92	21	1		

Table 4 Derived transformation and extinction coefficients. k and k' are primary and secondary extinction coefficients, respectively, while α and C are transformation coefficients.

Obs. Time	19.07.2012				
Indice	k	k'	α	C	
U	0.472 ± 0.031	-0.019 ± 0.033	-	-	-
B	0.326 ± 0.024	-0.057 ± 0.025	0.992 ± 0.038	0.745 ± 0.036	-
V	0.189 ± 0.007	-	-	-	-
$U - B$	-	-	0.861 ± 0.050	3.143 ± 0.046	-
$B - V$	-	-	0.077 ± 0.011	0.799 ± 0.017	-
Obs. Time	20.07.2012				
U	0.559 ± 0.033	-0.002 ± 0.035	-	-	-
B	0.392 ± 0.011	-0.037 ± 0.011	0.936 ± 0.018	0.786 ± 0.017	-
V	0.235 ± 0.002	-	-	-	-
$U - B$	-	-	0.813 ± 0.056	3.190 ± 0.054	-
$B - V$	-	-	0.051 ± 0.003	0.838 ± 0.005	-
Obs. Time	16.08.2012				
U	0.678 ± 0.030	-0.023 ± 0.067	-	-	-
B	0.525 ± 0.050	-0.246 ± 0.079	1.254 ± 0.105	0.550 ± 0.067	-
V	0.242 ± 0.007	-	-	-	-
$U - B$	-	-	0.836 ± 0.093	3.041 ± 0.043	-
$B - V$	-	-	0.084 ± 0.011	0.779 ± 0.016	-
Obs. Time	17.08.2012				
U	0.365 ± 0.026	0.216 ± 0.041	-	-	-
B	0.270 ± 0.041	0.002 ± 0.051	0.918 ± 0.066	0.890 ± 0.054	-
V	0.166 ± 0.004	-	-	-	-
$U - B$	-	-	0.537 ± 0.055	3.453 ± 0.034	-
$B - V$	-	-	0.081 ± 0.011	0.879 ± 0.015	-
Obs. Time	08.08.2013				
U	0.397 ± 0.014	0.007 ± 0.018	-	-	-
B	0.240 ± 0.014	-0.041 ± 0.015	0.972 ± 0.024	0.481 ± 0.021	-
V	0.118 ± 0.003	-	-	-	-
$U - B$	-	-	0.840 ± 0.027	2.893 ± 0.020	-
$B - V$	-	-	0.070 ± 0.003	0.538 ± 0.005	-

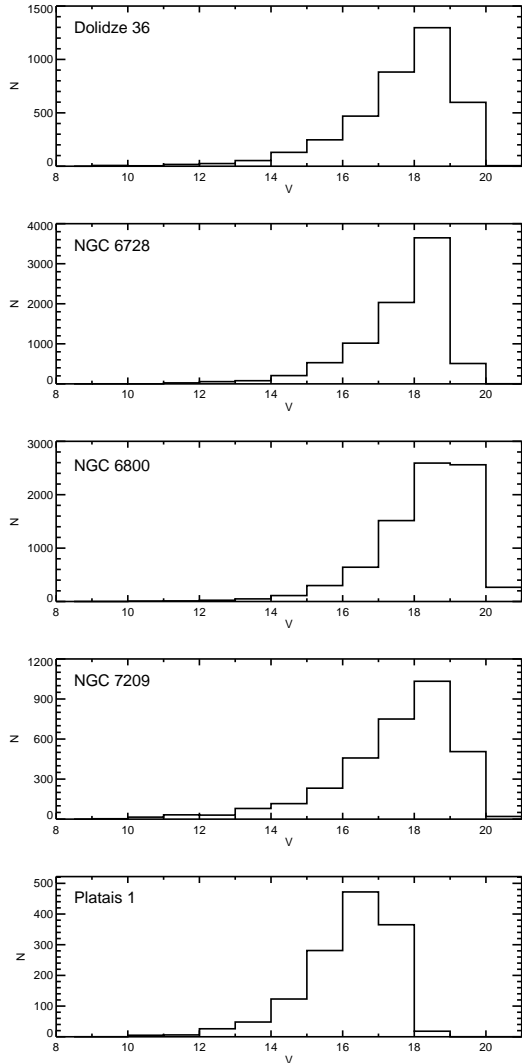


Fig. 2 Histograms of the V -band magnitudes measured for five clusters. Photometric completeness limits of the data are 19 mag for Dolidze 36, NGC 6728, NGC 6800, and NGC 7209, and 17 mag for Platais 1.

3 Data Analysis

3.1 Photometry of the detected objects

We constructed catalogues including all the sources in the field of view of five open clusters. All photometric catalogues of the open clusters are given electronically. In these catalogues, we present equatorial coordinates, apparent magnitude (V), colours ($U-B$, $B-V$), proper motion components ($\mu_\alpha \cos \delta$, μ_δ ; Roeser et al. 2010) and the probability of membership (P), respectively.

We listed mean errors of the measurements in the V band, and $U-B$ and $B-V$ colours in the selected apparent V magnitude ranges in Table 5. Errors at brighter ranges (mostly $V < 17$ mag) are relatively

small however, they increase exponentially towards fainter objects. To calculate the precise astrophysical parameters of the clusters, it is important to know the photometric completeness limit of the data. In order to determine this limit, we composed histograms of V magnitudes for each cluster (given in Fig. 2). Modes of the distribution of V magnitudes vary from 17 to 19 for the clusters used in this study. Platais 1 has a brighter limit of 17 mag since we took into account only observations with short exposure times. Only the calculations including stars brighter than the found completeness limits will be able to offer reliable results in the determination of the astrophysical parameters of the clusters.

Dolidze 36 was observed within the scope of the Sloan Digital Sky Survey (SDSS; York et al. 2000). In order to figure out reliability of our photometry we compared UBV observations with those calculated from SDSS. A cross-match of our catalogue of Dolidze 36 with SDSS Data Release 12 (DR12, Alam et al. 2015) resulted in 370 stars. V magnitudes of these common stars are ranging between 14 and 19 because SDSS photometry aims towards faint stars. We used relations of Chonis & Gaskell (2008) to transform $ugriz$ magnitudes to UBV . We show the comparison of observational and calculated V magnitude and $U-B$ and $B-V$ colours in Fig. 3. We obtained means and standard deviations of the magnitude and the colours from the differences as $\Delta_V = 0.088$, $\sigma_V = 0.086$, $\Delta_{U-B} = 0.140$, $\sigma_{U-B} = 0.191$ and $\Delta_{B-V} = -0.048$, $\sigma_{B-V} = 0.079$ mag. It is seen that zero points between the two systems for V and $B-V$ are usually small with very small standard deviations while they are somewhat larger for $U-B$. This large scattering in $U-B$ may arise from errors in the transformation since it is considered that the equations of Chonis & Gaskell (2008) do not take into account population types of the stars (Bilir et al. 2008, 2011).

3.2 Cluster radius and radial stellar surface density

Since the studied open clusters show no noticeable central concentration except Platais 1 with little central concentration, we were only able to estimate the stellar density profile for Platais 1 using stars with magnitudes brighter than the photometric completeness limit, $V = 17$ mag. The central coordinates of the cluster were assumed to be as given in the WEBDA database⁵ ($\alpha_{2000.0} = 21^h 30^m 02^s$, $\delta_{2000.0} = +48^\circ 58' 36''$). The stellar density values for the main-sequence sample of the cluster have been evaluated in 1 arcminute steps. The last two annuli had a width of 2 arcmin because of a significant decrease in the number of stars (see, Fig. 4).

⁵<http://webda.physics.muni.cz>

Table 5 Mean errors of the photometric measurements for the stars in the directions of five open clusters. N represents the number of stars within the V apparent magnitude range given in the first column.

V range	Dolidze 36			NGC 6728			NGC 6800			NGC 7209			Platais 1			
	N	σ_V	σ_{U-B}	σ_{B-V}	N	σ_V	σ_{U-B}	σ_{B-V}	N	σ_V	σ_{U-B}	σ_{B-V}	N	σ_V	σ_{U-B}	σ_{B-V}
(8, 10]	7	0.001	0.002	0.001	1	0.002	0.002	0.002	—	—	—	—	3	0.001	0.002	0.001
(10, 12]	21	0.002	0.003	0.002	24	0.007	0.022	0.009	19	0.002	0.002	0.002	47	0.002	0.002	0.002
(12, 14]	78	0.004	0.014	0.008	133	0.013	0.050	0.016	72	0.004	0.011	0.007	110	0.004	0.007	0.005
(14, 16]	377	0.003	0.010	0.005	735	0.006	0.029	0.008	409	0.004	0.014	0.006	348	0.004	0.007	0.005
(16, 18]	1351	0.009	0.039	0.016	3048	0.021	0.093	0.026	2157	0.014	0.045	0.020	1208	0.012	0.023	0.016
(18, 20]	1895	0.029	0.108	0.054	4155	0.054	0.192	0.067	5153	0.048	0.122	0.074	1539	0.036	0.075	0.049
(20, 22]	5	0.076	—	0.152	3	0.186	0.184	0.202	268	0.117	0.224	0.181	20	0.095	0.289	0.144

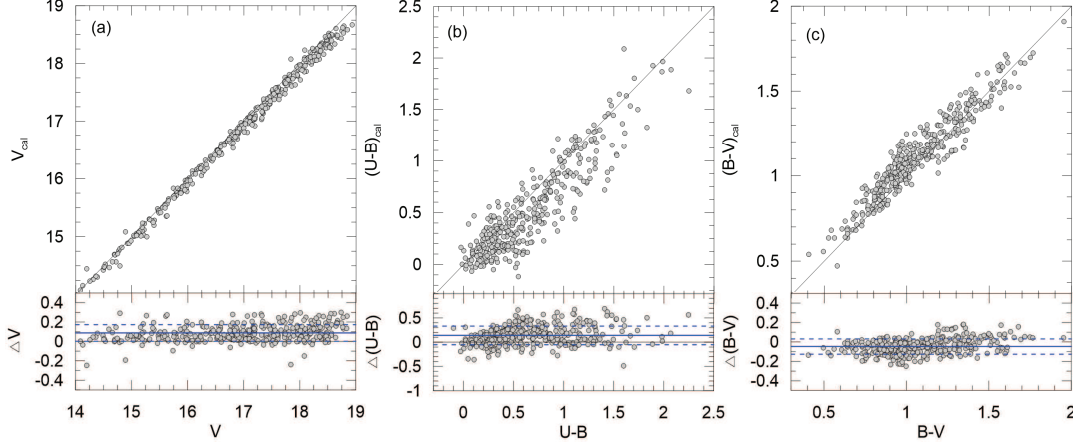


Fig. 3 Comparisons of observational magnitudes and colours with those calculated from SDSS DR12 (Alam et al. 2015).

We fitted the King (1962) model to the observed radial density profile and used a χ^2 minimization technique to determine structural parameters. The best fit to the density profile is shown with a solid line in Fig. 4. We found the central stellar density, core radius of the cluster, and the background stellar density as $f_0 = 2.43 \pm 0.25$ stars arcmin $^{-2}$, $r_c = 2.10 \pm 0.75$ arcmin and $f_{bg} = 2.16 \pm 0.27$ stars arcmin $^{-2}$, respectively.

Turner et al. (1994) estimated the stellar density profile of Platais 1 for the limiting R -band magnitude 17, using a photographic enlargement of the Palomar Observatory Sky Survey (POSS) E-plate. They only reported the background stellar density as $f_{bg} = 4.38 \pm 0.13$ stars arcmin $^{-2}$. To infer their central stellar density and core radius of the cluster, we digitized values of their density profile from their figure and then fitted them with the King model (King 1962). As a result, the central stellar density and the core radius of the cluster were found as $f_0 = 3.25$ stars arcmin $^{-2}$ and $r_c = 3.20$ arcmin, respectively. The core radius of the cluster is in agreement with the one in Turner et al. (1994) within the quoted error, but the other parameters are a little different from each other. The reason for this incompatibility may be due to the data taken

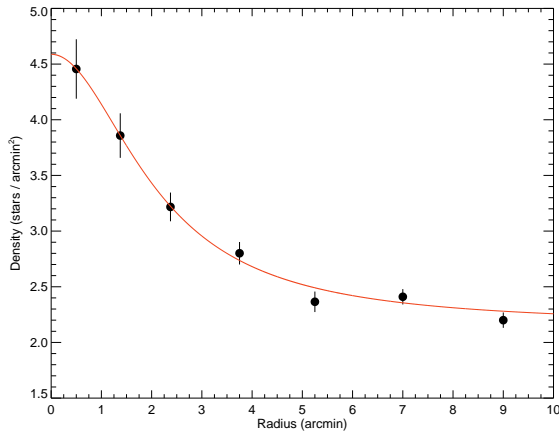


Fig. 4 Stellar density profile of Platais 1. Errors were determined from sampling statistics, \sqrt{N} , where N is the number of stars used in the density estimation.

in different bands, effecting the number of stars used for the estimation.

3.3 CMDs and membership probabilities

CMDs are robust tools to determine the parameters of the open clusters. However, in order to be able to use CMDs as tools to determine physical parameters of the clusters one should first make sure that the stars in the diagram are actual members of the cluster in question. Therefore, a process to determine the membership probabilities (P) of each star in the field is necessary. We calculated this membership probability of all the objects in the field of view using the method given by Balaguer-Núñez et al. (1998). This method takes into account the errors of the stellar proper motions as well as the average cluster proper motion, and uses the kernel estimation technique to obtain distribution of the data.

PPMXL (Roeser et al. 2010) and UCAC4 (Zacharias et al. 2013) are the most often used catalogues of positions and proper motions. PPMXL is the largest catalogue containing about 900 million objects reaching apparent magnitudes down to $V = 20$. The UCAC4 is a more recent and precise catalogue containing about 113 million stars reaching magnitudes down to $R = 16$. In this study we collect proper motion components of individual stars from the PPMXL due to the magnitude limit and the larger number of stars. In order to check the used proper motions with those from the literature, we calculated the differences of the absolute proper motions for all five cluster to the values listed in Kharchenko et al. (2013). The differences range from 1.7 to 5.4 mas yr⁻¹ which is well within the error ranges of the individual proper motions. Consequently, we found excellent agreement with those of the algorithm published by Javakhishvili et al. (2006). We calculated the mean and median of the differences of both methods which range between 7 and 12% for the five open clusters. This excellent agreement is likely due to the distance of the clusters ($d > 1$ kpc) at which both algorithm easily find non-members because of their much larger proper motions than the cluster members. The histogram of the differences efficiently discriminates the members of the cluster from the non-members. In order to identify the most likely members of each cluster, we fitted the zero-age main sequence (ZAMS) of Sung et al. (2013) for solar metallicity to the $V \times (B - V)$ CMDs using only the main-sequence stars with $P \geq 50\%$. Although all stars with $P \geq 50\%$ in the field of view show a large scatter in CMDs (orange crosses in Fig. 5), the method is efficient in determination of main sequence of the clusters. We also

shifted the fitted main sequence to brighter V magnitudes to take into account the effect of binary stars (see Fig. 5). Finally, we assumed that the stars with $P \geq 50\%$ within this band-like region are the most likely main-sequence members of the clusters. The red dots outside the main-sequence band in Fig. 5 indicate that some stars with $P \geq 50\%$ have already left the ZAMS. These stars correspond to the turn-off points of the clusters. We assume that these objects are likely members of the clusters, as well. For further analysis, we considered the stars identified with this procedure for each cluster.

4 Astrophysical parameters of the clusters

The determination of astrophysical parameters by using methods that are independent of each other has been successfully applied in many of our previous studies (Bilir et al. 2010; Bostancı et al. 2015; Ak et al. 2016; Bilir et al. 2016). In this section, astrophysical parameters of the five open clusters, such as reddening, metallicities, distance moduli and ages, are determined via fitting models to the observed data points selected following the method described in Section 3.3.

4.1 The reddening

We used the TCD constituted from the most probable main-sequence stars, in order to derive the colour excess of each cluster. We compared the $(U - B) \times (B - V)$ TCD of these stars with the ZAMS of Sung et al. (2013) for solar metallicity using the following equation (Garcia et al. 1988)

$$E(U - B) = 0.72 \times E(B - V) + 0.05 \times E(B - V)^2, \quad (1)$$

and estimated the $E(B - V)$ and $E(U - B)$ colour excesses by shifting de-reddened ZAMS curve with steps of 0.01 mag within the range $0 < E(B - V) \leq 1$ mag until the best fit is achieved with the TCD of each cluster as shown in Fig. 6. We took into account stars with $\sigma_{U-B} < 0.1$ mag for Dolidze 36, NGC 6728, NGC 6800, and NGC 7209, and $\sigma_{U-B} < 0.06$ mag for Platais 1. Results are given in Table 6. The errors were calculated by shifting the best fit curve for $\pm 1\sigma$.

4.2 Metallicities of the clusters

We measured the photometric metallicity of the clusters following a method based on F-G type main-sequence stars (Karaali et al. 2011). Therefore, we considered

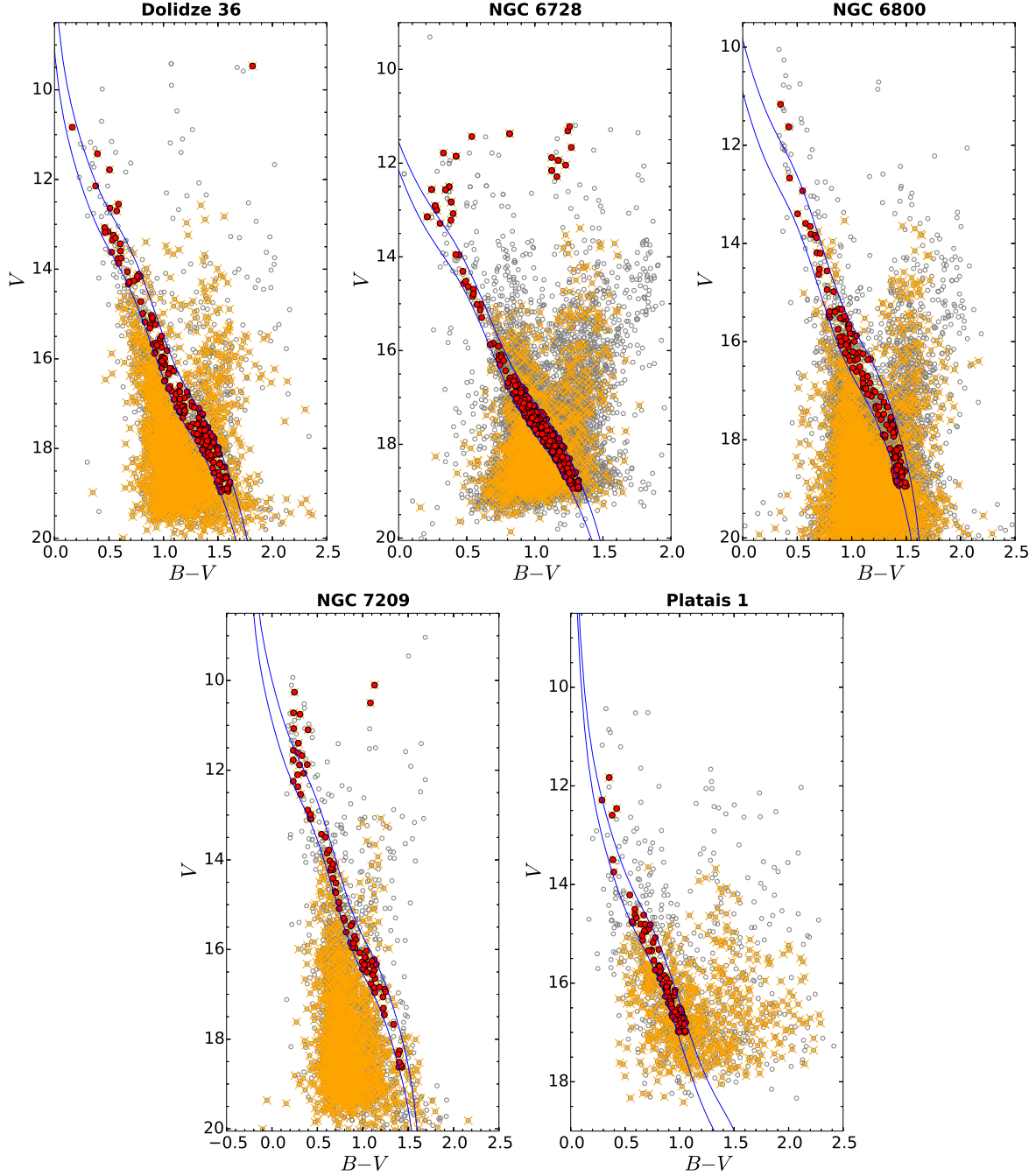


Fig. 5 $V \times (B - V)$ CMDs of the five clusters. Solid lines represent the ZAMS of Sung et al. (2013) and the one shifted to the brighter V magnitudes for taking into account binary stars. Red dots indicate the most probable cluster stars within this band-like region while orange crosses represent the stars with $P \geq 50\%$ in the field of view.

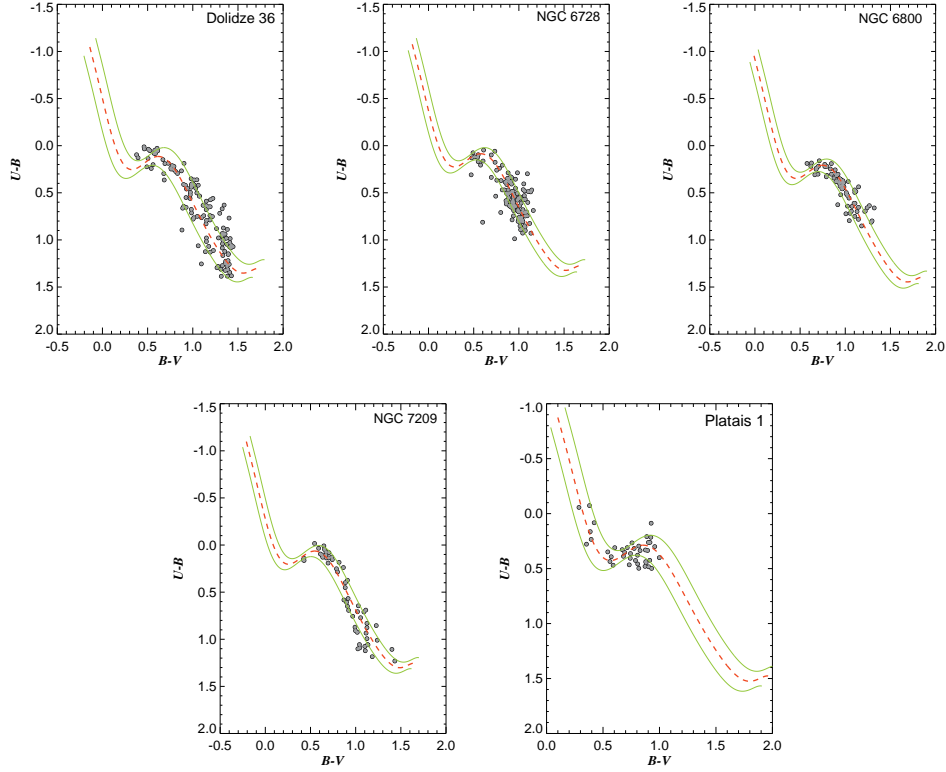


Fig. 6 $(U - B) \times (B - V)$ TCDs for the main-sequence stars for each cluster. Red dashed lines are the reddened ZAMS of Sung et al. (2013) fitted to cluster stars and green solid lines represent $\pm 1\sigma$ standard deviations, respectively.

F0-G0 spectral type main-sequence stars with a membership probability $P \geq 50\%$ and with colours $0.3 \leq (B - V)_0 \leq 0.6$ mag (Cox 2000). We selected six stars in Dolidze 36, and NGC 6728, 12 stars in NGC 6800, 13 stars in NGC 7209, and 10 stars in Platais 1.

For this method we first need to calculate normalised ultraviolet (UV) excesses, which is the difference between a star’s de-reddened $(U - B)_0$ colour index and the one corresponding to the members of the Hyades cluster with the same de-reddened $(B - V)_0$ colour index ($\delta = (U - B)_{0,H} - (U - B)_{0,S}$, where H and S denote to Hyades and star, respectively). Thus, we calculated the normalised UV-excesses of member stars for each cluster and normalised their δ differences to the UV-excess at $(B - V)_0 = 0.6$ mag (i.e. $\delta_{0.6}$). The distributions of normalised $\delta_{0.6}$ UV-excesses were fitted with a Gaussian function and we adopt the Gaussian peak as result for each cluster. The $(U - B)_0 \times (B - V)_0$ TCDs and histograms of the normalised $\delta_{0.6}$ UV-excesses of the selected stars are shown in Fig. 7. The standard deviation of the metallicity distribution for each cluster was assumed as the uncertainty of the metallicity.

The $[\text{Fe}/\text{H}]$ metallicity for each cluster was calculated from the following equation (Karaali et al. 2011):

$$[\text{Fe}/\text{H}] = 0.105 - 3.557 \times \delta_{0.6} - 14.316 \times \delta_{0.6}^2. \quad (2)$$

To transform the $[\text{Fe}/\text{H}]$ metallicities to the mass fraction Z of all elements heavier than helium, we used the following equations from Bovy who obtained them analytically using PARSEC isochrones ⁶:

$$Z_X = 10^{[\text{Fe}/\text{H}] + \log\left(\frac{Z_\odot}{1 - 0.248 - 2.78 \times Z_\odot}\right)}, \quad (3)$$

and

$$Z = \frac{(Z_X - 0.2485 \times Z_X)}{(2.78 \times Z_X + 1)}. \quad (4)$$

Here, Z_X is the intermediate operation function depending on $[\text{Fe}/\text{H}]$ and the solar mass fraction is taken as $Z_\odot = 0.0152$ (Bressan et al. 2012). Resulting Z value for each cluster is presented in Table 6.

⁶<https://github.com/jobovy/isodist/blob/master/isodist/Isochrone.py>

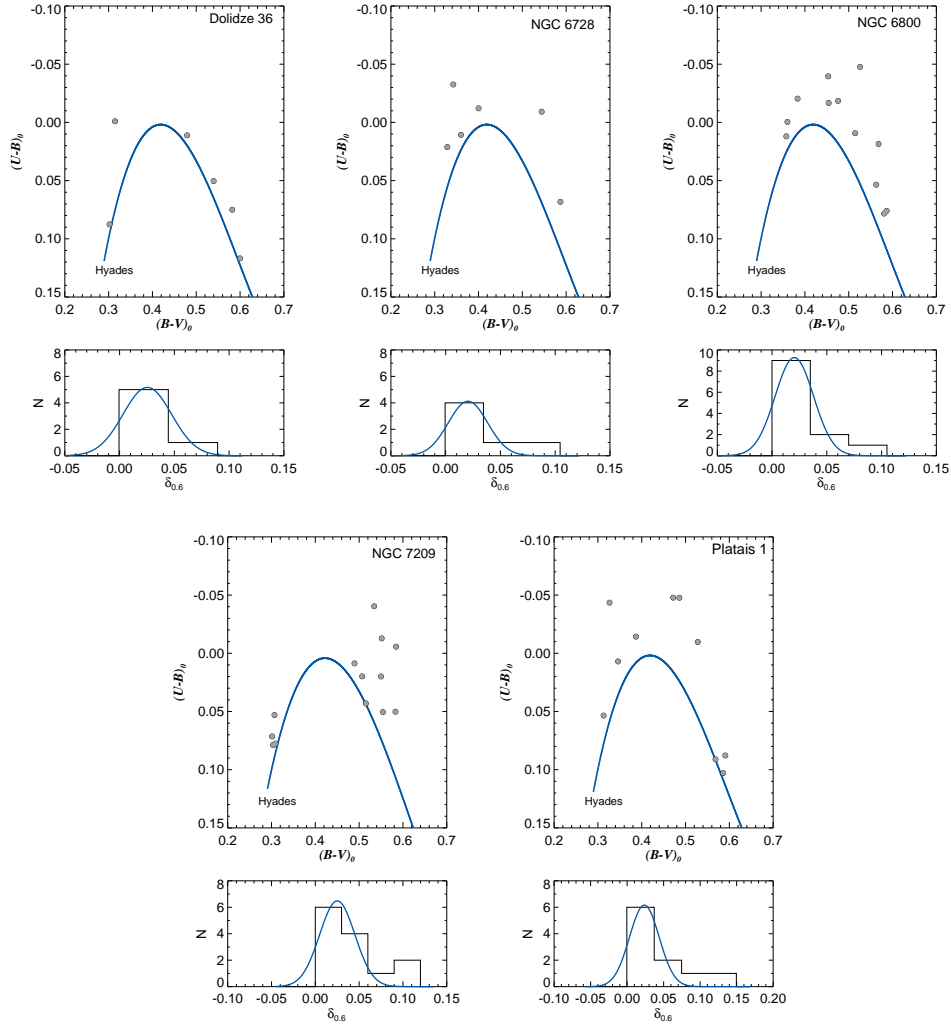


Fig. 7 $(U - B)_0 \times (B - V)_0$ TCDs (upper panel) and the histograms (lower panel) for the normalized UV-excesses for main-sequence stars used for the metallicity estimation of five open clusters. The solid lines in the upper and lower panels represent the main-sequence of Hyades cluster and the Gaussian fit to the histogram, respectively.

4.3 Distance moduli and the ages of the clusters

Using the reddening and metallicity values that we calculated above, we employed the isochrone fitting procedure to simultaneously obtain distance moduli and ages of the five open clusters. We shifted the theoretical isochrones provided by the PARSEC V1.2 synthetic stellar library (Bressan et al. 2012; Tang et al. 2014; Chen et al. 2014) onto observed $V \times (U - B)$ and $V \times (B - V)$ CMDs, respectively. Fig. 8 shows CMDs of each cluster overplotted with the best fit theoretical isochrones. In the $V \times (B - V)$ CMD of Dolidze 36 (Fig. 8), some stars with most likely membership located in the $0.4 < B - V < 0.6$ and $11 < V < 13$ magnitudes are not fitted well with the isochrone. The reason for this could be that these redder stars are binary stars.

We assumed the standard selective absorption coefficient as $R_V = 3.1$ (Schultz & Wiemer 1975) for the distance calculation. We considered the errors in distance moduli of the clusters for the determination of errors in the distances (see also, Carraro et al. 2017). We listed the resulting distance moduli, distances and ages of the clusters in Table 6.

4.4 Mass functions of the clusters

Mass function (MF) indicates the relative number of stars in a unit range of mass and denotes the rate of star formation based on stellar mass. Considering the most likely main-sequence members of the open clusters in this study, we first calculated M_V of each star using the distance moduli and V magnitudes. We then

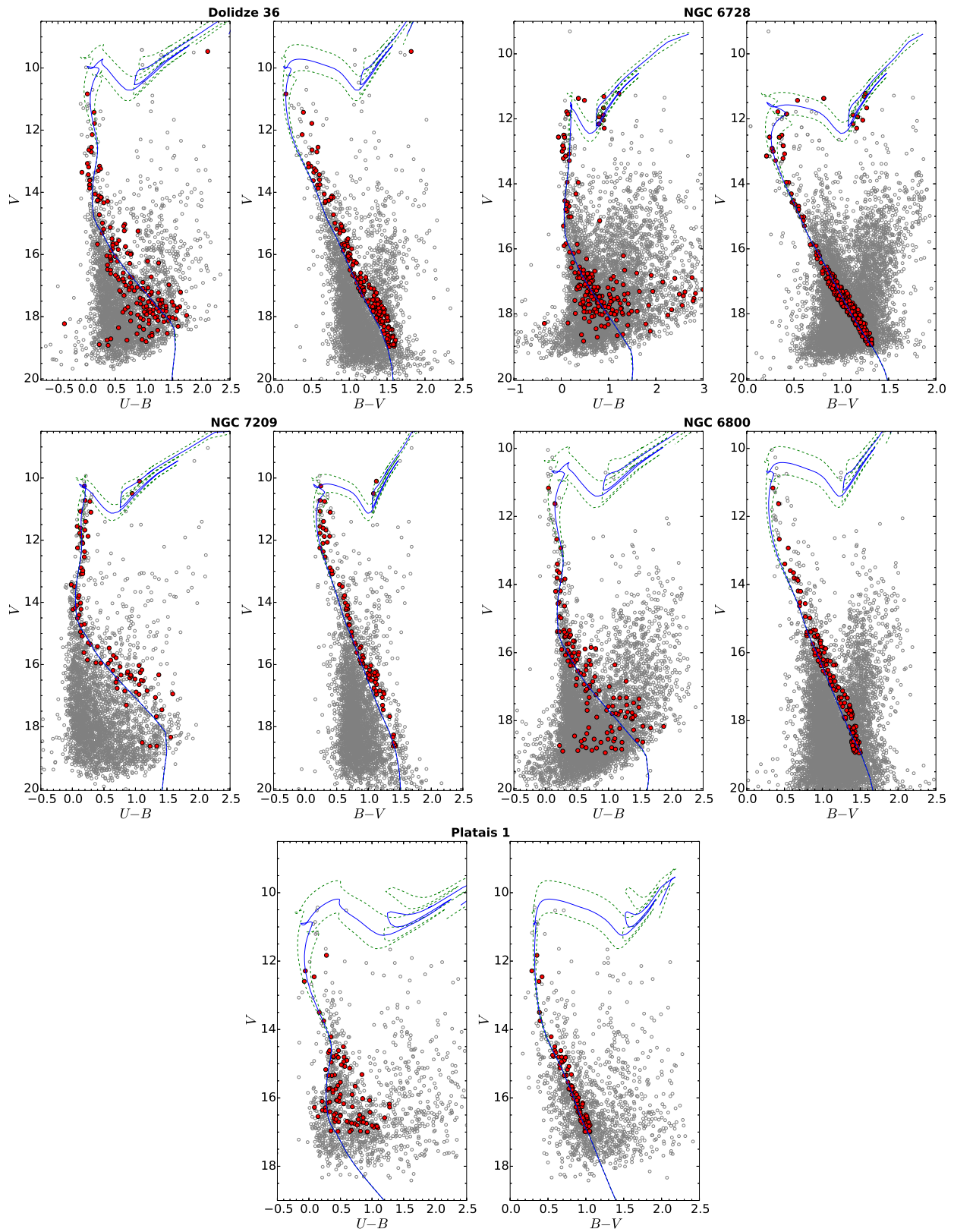


Fig. 8 $V \times (U - B)$ and $V \times (B - V)$ CMDs for the five open clusters. Red circles denote the most probable members of each cluster. Blue lines are the best fit theoretical isochrones determined in this study. The green dashed lines represent the isochrones with estimated age plus/minus its error.

Table 6 Colour excesses ($E(B - V)$), distance moduli (μ_V), distances (d) iron abundances ($[Fe/H]$) metallicities (Z) and ages (t) estimated using two CMDs and TCDs of each cluster.

Cluster	$E(B - V)$ (mag)	μ_V (mag)	d (pc)	$[Fe/H]$ (dex)	Z	t (Myr)
Dolidze 36	0.19 ± 0.06	10.70 ± 0.19	1050 ± 90	0.00 ± 0.09	0.0152 ± 0.0036	400 ± 100
NGC 6728	0.15 ± 0.05	11.50 ± 0.25	1610 ± 190	0.02 ± 0.11	0.0159 ± 0.0042	750 ± 150
NGC 6800	0.32 ± 0.05	11.40 ± 0.26	1210 ± 150	0.03 ± 0.07	0.0162 ± 0.0027	400 ± 100
NGC 7209	0.12 ± 0.04	10.50 ± 0.18	1060 ± 90	0.01 ± 0.08	0.0154 ± 0.0032	600 ± 100
Platais 1	0.43 ± 0.06	12.50 ± 0.29	1710 ± 250	0.01 ± 0.08	0.0154 ± 0.0032	175 ± 50

converted M_V to mass values using the best fit theoretical PARSEC isochrones for each cluster. Fig. 9 shows MFs of the five open clusters. We derived the slope x of mass function from the following linear relation: $\log(dN/dM) = -(1 + x) \times \log(M) + C$, where dN indicates the number of stars in a mass bin dM with central mass of M , and C is a constant. We give the resulting values for the slopes of MFs for each cluster in Table 7.

4.5 Integrated magnitudes and colours of the clusters

We used the following equation to convert apparent magnitudes and absolute magnitudes in UBV passbands to flux values for the stars with the membership probability $P > 0\%$ in order to not to miss member stars of open clusters and then summed flux of all these stars to obtain U , B , V , and M_V integrated magnitudes ($I(m)$) of the clusters:

$$I(m) = -2.5 \times \log \left[\sum_i (10^{-0.4 \times m_i}) \right]. \quad (5)$$

From reddening and distance moduli values (see Table 6), we calculated the integrated magnitude, colours, and absolute magnitude of each cluster and listed them in Table 8.

Lata et al. (2002) found relations between integrated parameters and ages using 352 open clusters. We also calculated the integrated $I(B - V)_0$ and $I(M_V)$ values with their relations given below:

$$I(B - V)_0 = 1.99 - 0.79 \times (\log t) + 0.07 \times (\log t)^2, \quad (6)$$

Table 7 The slopes of the mass functions of clusters.

Cluster	N	x	Mass range
Dolidze 36	122	-1.39 ± 0.91	$0.7 < M/M_\odot < 1.7$
NGC 6728	182	-1.58 ± 0.61	$0.7 < M/M_\odot < 1.9$
NGC 6800	110	-1.58 ± 0.50	$0.7 < M/M_\odot < 1.9$
NCG 7209	60	-1.31 ± 0.35	$0.7 < M/M_\odot < 1.8$
Platais 1	40	-1.49 ± 0.59	$1.3 < M/M_\odot < 2.1$

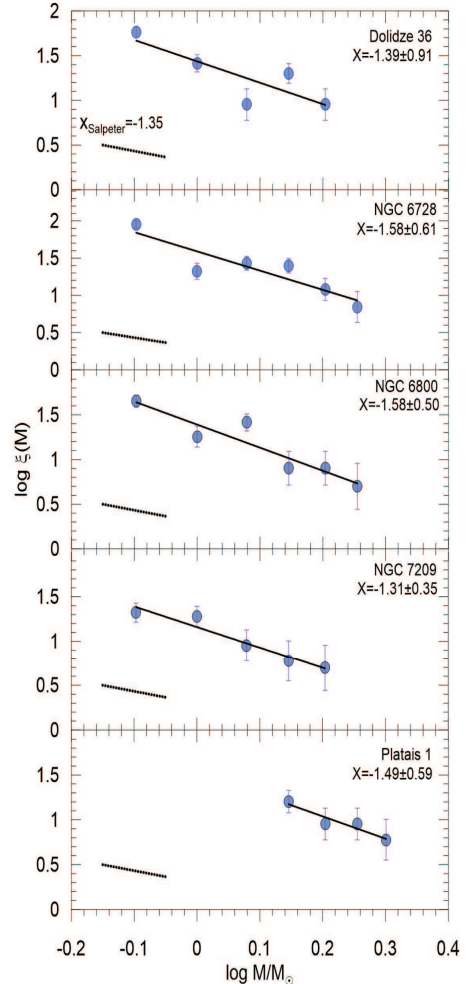


Fig. 9 Mass functions of clusters determined from the stars with the membership probability $P \geq 50\%$.

$$I(M_V) = -36.53 + 6.90 \times (\log t) - 0.36 \times (\log t)^2, \quad (7)$$

where t indicates the age of the cluster. All in all, when we compare our integrated colour and absolute magnitudes calculated from the stars located in the direction of clusters with those calculated using Eqs. (6) and (7) from Lata et al. (2002), we see that they are in good agreement except Dolidze 36, as seen in Table 8. When we look over the large samples of Lata et al. (2002), a few of them have similar colour and absolute magnitude values with Dolidze 36. These values are in the scattered region of Fig. 4 given by Lata et al. (2002), since Dolidze 36 has fainter and redder magnitudes than the other clusters. The most likely reason is that, in a cluster, as the massive stars evolve the dynamical evolution produces mass segregation (Nilakshi et al. 2002).

5 Discussion and Conclusions

This work presents the fundamental parameters of five open clusters, namely Dolidze 36, NGC 6728, NGC 6800, NGC 7209, and Platais 1, obtained from CCD *UBV* observations, which were analysed in detail. Astrometric data were used to calculate the membership probabilities of the stars in the field of view of each cluster. We took into account the most probable member stars of the clusters to determine precisely the astrophysical parameters of each cluster.

Simultaneous determination of astrophysical parameters by fitting the theoretical stellar evolutionary isochrones to the observed CMDs can suffer from the reddening-age degeneracy (Anders et al. 2004; King et al. 2005; Bridžius et al. 2008; de Meulenaer et al. 2013; Janes et al. 2014). Therefore, we independently found the parameters of the clusters. The distances and ages of the clusters were derived by fitting TCDs and CMDs with the theoretical PARSEC models (Bressan et al. 2012) while metallicities of the clusters were obtained using the method given by Karaali et al. (2011), based on F0-G0 spectral type main-sequence stars (Cox 2000). This strategy allows us to reduce in part the effect of the reddening-age degeneracy on the parameters. Results of the cluster parameters are given in Table 6. As specified before, the clusters in our sample have only a few studies in the literature. Previous results are listed in Table 1.

5.1 Dolidze 36

The reddening, the distance modula, the distance, the metallicity and the age of Dolidze 36 were obtained

as $E(B - V) = 0.19 \pm 0.06$ mag, $\mu_V = 10.70 \pm 0.19$ mag, $d = 1050 \pm 90$ pc, $[\text{Fe}/\text{H}] = +0.00 \pm 0.09$ dex, and $t = 400 \pm 100$ Myr, respectively. Dolidze 36 is one of the clusters poorly studied in literature. Our reddening value agrees within the quoted errors with the value in the catalogue given by Kharchenko et al. (2005). However, our distance is larger and age is somewhat younger when comparing those from Kharchenko et al. (2005).

5.2 NGC 6728

The reddening, the distance modula, the distance, the metallicity and the age of NGC 6728 were determined as $E(B - V) = 0.15 \pm 0.05$ mag, $\mu_V = 11.50 \pm 0.25$ mag, $d = 1610 \pm 190$ pc, $[\text{Fe}/\text{H}] = +0.02 \pm 0.11$ dex, and $t = 750 \pm 150$ Myr, respectively. There is only one previous study for the cluster by Kharchenko et al. (2005), who determined cluster parameters using the isochrones with solar metallicity ($Z = 0.019$) in their catalogues. Our values for reddening and age agree within the quoted errors, but the distance modula and the distance from this study are slightly larger than their results (see Table 1).

5.3 NGC 6800

The reddening, the distance modula, the distance, the metallicity and the age of NGC 6800 are $E(B - V) = 0.32 \pm 0.05$ mag, $\mu_V = 11.40 \pm 0.26$ mag, $d = 1210 \pm 150$ pc, $[\text{Fe}/\text{H}] = +0.03 \pm 0.07$ dex, and $t = 400 \pm 100$ Myr, respectively. Ananjevskaia et al. (2015) studied NGC 6800 comprehensively using photographic plates from the Pulkovo “Fantasy” automated measuring system and point source catalogue (Cutri et al. 2003) of Two Micron All Sky Survey (2MASS, Skrutskie et al. 2006). They obtained the parameters of the cluster from 109 member stars in $V \times (B - V)$ and $J \times (J - K_S)$ CMDs. Our results do not seem to be in agreement with their results. Their reddening value is slightly larger than ours while the distance modula, distance and age are smaller than our results. The difference could be attributed to the quality of their data (photographic plates) and the method they used. Kharchenko et al. (2005) gave the parameters of the cluster in their catalogue, as well. Only the age of the cluster is in good agreement with our value.

5.4 NGC 7209

The reddening, the distance modula, the distance, the metallicity and the age of NGC 7209 were found as $E(B - V) = 0.12 \pm 0.04$ mag, $\mu_V = 10.50 \pm 0.18$ mag, $d = 1060 \pm 90$ pc, $[\text{Fe}/\text{H}] = +0.01 \pm 0.08$ dex, and $t = 600 \pm 100$

Table 8 Integrated absolute magnitudes and colours of the clusters.

Cluster	This study				Lata et al. (2002)		Differences	
	$I(V_0)$	$I(U - B)_0$	$I(B - V)_0$	$I(M_V)$	$I(B - V)_0$	$I(M_V)$	$\Delta I(B - V)_0$	$\Delta I(M_V)$
Dolidze 36	6.713	0.279	0.811	-3.398	0.374	-3.814	0.437	0.416
NGC 6728	7.337	0.220	0.511	-3.699	0.492	-3.648	0.019	-0.051
NGC 6800	6.588	-0.037	0.320	-3.819	0.374	-3.814	-0.054	-0.005
NGC 7209	6.470	0.177	0.362	-3.657	0.449	-3.701	-0.087	0.044
Platais 1	7.090	0.037	0.329	-4.077	0.234	-4.114	0.095	0.037

Myr, respectively. NGC 7209 has a number of previous studies (Kharchenko et al. 2005; Vasevicius et al. 1997; Malysheva 1997; Twarog et al. 1997; Lynga 1987; Claria et al. 1996; Piatti et al. 1995). We summarized early works in Table 1. Our reddening value is in agreement within the quoted errors with those of Kharchenko et al. (2005), Lynga (1987) Claria et al. (1996), and Piatti et al. (1995), but somewhat smaller than the value reported by Vasevicius et al. (1997), Malysheva (1997), and Twarog et al. (1997). Distance modula and distance in our study agree with the values from previous studies. On the other hand, we found the age of the cluster older than those in the literature. Our metallicity value agrees within the quoted errors with the value given by Twarog et al. (1997), but it is larger than those of Vasevicius et al. (1997) and Piatti et al. (1995).

5.5 Platais 1

The reddening, the distance modula, the distance, the metallicity and the age of Platais 1 are $E(B - V) = 0.43 \pm 0.06$ mag, $\mu_V = 12.50 \pm 0.29$ mag, $d = 1710 \pm 250$ pc, $[\text{Fe}/\text{H}] = +0.01 \pm 0.08$ dex, and $t = 175 \pm 50$ Myr, respectively. This is the youngest cluster with the largest reddening value at the farthest distance in our sample. There is only one photometric study on the cluster (Turner et al. 1994). The astrophysical parameters of the cluster in our study are well consistent with those from Turner et al. (1994) while the structural parameters are slightly in agreement.

Our sample consists of young open clusters (a mean value of ~ 500 Myr), which corresponds to an average time scale for dynamics to have not influence upon the IMF of the stellar systems (Sagar & Griffiths 1998; Sagar et al. 2001). Therefore, we can assume that MF of the clusters could be equivalent to their IMF. We derived the slopes of the mass functions for the member stars of each cluster, which have mass values ranging from 0.7 to 2.1 M/M_\odot . The MF slopes of the five open clusters vary between 1.31 and 1.58 (see Table 7), which are comparable to the value of 1.35 reported by Salpeter (1955) within the quoted errors. Additionally,

our calculations for integrated absolute magnitudes and colours are in agreement with those derived using relations of Lata et al. (2002).

6 Acknowledgments

We thank the anonymous referee for his/her insightful and constructive suggestions, which significantly improved the paper. This study has been supported in part by the Scientific and Technological Research Council (TÜBİTAK) 113F270. Part of this work was supported by the Research Fund of the University of Istanbul, Project Numbers: FDK-2016-22543 and BYP48482. We thank to TÜBİTAK for a partial support in using T100 telescope with project number 15AT100-738. We also thank to the on-duty observers and members of the technical staff at the TÜBİTAK National Observatory for their support before and during the observations.

References

- Ak, T., Bostancı, Z. F., Yontan, T., et al., 2016, *Ap&SS*, 361, 126
- Alam, S., Albareti, F. D., Allende Prieto, C., et al., 2015, *ApJS*, 219, 12
- Ananjevskaia, Yu. K., Frolov, V. N., Polyakov, E. V., 2015, *AstL*, 41, 334
- Anders, P., Bissantz, N., Fritze-v. Alvensleben, U., de Grijs, R., 2004, *MNRAS*, 347, 196
- Balaguer-Núñez, L., Tian, K.P., Zhao, J.L., 1998, *A&AS*, 133, 387
- Bertin, E., Arnouts, S., 1996, *A&AS*, 117, 393
- Bica, E., Bonatto, Ch., Blumberg, R., 2006, *A&A* 460, 83
- Bilir, S., Ak, S., Karaali, S., Cabrera-Lavers, A., Chonis, T. S., Gaskell, C. M., 2008, *MNRAS*, 384, 1178
- Bilir, S., Güver, T., Khamitov, I., Ak, T., Ak, S., Coşkunoglu, K. B., Paunzen, E., Yaz, E., 2010, *Ap&SS*, 326, 139
- Bilir S., Karaali S., Ak S., Dağtekin N. D., Önal Ö., Yaz E., Coşkunoglu B., Cabrera-Lavers A., 2011, *MNRAS*, 417, 2230
- Bilir, S., Bostancı, Z. F., Yontan, T., et al., 2016, *AdSpR*, 58, 1900
- Bridžius, A., Narbutis, D., Stonkutė, R., Deveikis, V., Vansevicius, V., 2008, *BaltA*, 17, 337
- Bostancı Z.F., Ak, T., Yontan, T., et al., 2015, *MNRAS*, 453, 1095
- Bressan, A., Marigo, P., Girardi, L., Salasnich, B., Dal Cero, C., Rubele, S., Nanni, A., 2012, *MNRAS*, 427, 127
- Carraro, G., Sales Silva, J. V., Moni Bidin, C., Vazquez, R. A., 2017, *AJ*, 153, 99.
- Chen, Y., Girardi, L., Bressan, A., Marigo, P., Barbieri, M., Kong, X., 2014, *MNRAS*, 444, 2525
- Chonis, T. S., Gaskell, C. M., 2008, *AJ*, 135, 264
- Claria, J. J., Piatti, A. E., Osborn, W., 1996, *PASP*, 108, 672
- Cox, A. N., 2000. *Allen's astrophysical quantities*, 4th ed. Publisher: New York: AIP Press; Springer, 2000. Edited by Arthur N. Cox. ISBN: 0387987460
- Cutri, R. M., et al., 2003, *2MASS All-Sky Catalog of Point Sources*, CDS/ADC Electronic Catalogues, 2246
- de Meulenaer, P., Narbutis, D., Mineikis, T., Vancsevicius, V., 2013, *A&A*, 550, 20
- Garcia, B., Claria, J. J., Levato, H., 1988, *Ap&SS*, 143, 317
- Janes K., Hoq S., 2013, *AJ*, 141, 92
- Janes, K., Barnes, S. A., Meibom, S., Hoq, S., 2014, *AJ*, 147, 139
- Javakhishvili, G., Kukhianidze, V., Todua, M., Inasaridze, R., 2006, *A&A*, 447, 915
- Karaali, S., Bilir, S., Ak, S., Yaz, E., Coşkunoglu, B., 2011, *PASA*, 28, 95
- King I., 1962, *AJ*, 67, 471
- King, I.R., Bedin, L.R., Piotto, G., Cassisi, S., Anderson, J., 2005, *AJ*, 130, 626
- Kharchenko, N. V., Piskunov, A. E., Roeser, S., Schilbach, E., Scholz, R. -D., 2005, *A&A*, 438, 1163
- Kharchenko, N. V., Piskunov, A. E., Schilbach, E., Roeser, S., Scholz, R. -D., 2013, *A&A*, 558A, 53
- Landolt, A.U., 2009, *AJ*, 137, 4186
- Lang, D., Hogg, D. W., Mierle, K., Blanton, M., Roweis, S., 2010, *AJ*, 139, 1782
- Lata, S., Pandey, A. K., Sagar, R., Mohan, V., 2002, *A&A*, 388, 158
- Lynga, G., 1987, *Catalogue of open cluster data*, 5th Ed., FEB 1987, Lund Observatory, Sweden
- Roeser, S., Demleitner, M., Schilbach, E., 2010, *AJ*, 139, 2440
- Malysheva, L. K., 1997, *AstL*, 23, 585
- Nilakshi, S. R., Pandey, A. K., Mohan, V., 2002, *A&A*, 383, 153
- Piatti, A. E., Claria, J. J., Abadi, M. G., 1995, 110, 2813
- Sagar, R., Griffiths, W. K., 1998, *MNRAS*, 299, 777
- Sagar, R., Munari, U., de Boer, K. S., 2001, *MNRAS*, 327, 23S
- Salpeter, E. E., 1955, *ApJ*, 121, 161
- Schultz, G. V., Wiemer, W., 1975, *A&A*, 43, 133
- Skrutskie, M. F., et al., 2006, *AJ*, 131, 1163
- Sung, H., Lim, B., Bessell, M.S., Kim, J. S., Hur, H., Chun, M., Park, B., 2013, *JKAS*, 46, 103
- Tang, J., Bressan, A., Rosenfield, P., Slemmer, A., Marigo, P., Girardi, L., Bianchi, L., 2014, *MNRAS*, 445, 4287
- Turner, D. G., Mandushev, G. I., Forbes, D., 1994, *AJ*, 107, 1796
- Twarog, B. A., Ashman, K. M., Anthony-Twarog, B. J., 1997, *AJ*, 114, 2556
- Vansevicus, V., Platais, I., Paupers, O., Abolins, E., 1997, *MNRAS*, 285, 871
- Yontan, T., Bilir, S., Bostancı, Z. F., et al., 2015, *Ap&SS*, 355, 267
- York, D. G., Adelman, J., Anderson, J. E., et al., 2000, *AJ*, 120, 1579
- Zacharias, N., Finch, C. T., Girard, T. M., Henden, A., Bartlett, J. L., Monet, D. G., Zacharias, M. I., 2013, *AJ*, 145, 44